ORIGINAL RESEARCH

Folate-targeted docetaxel-lipid-based-nanosuspensions for active-targeted cancer therapy

Lili Wang
Min Li
Na Zhang

School of Pharmaceutical Science,
Shandong University, Jinan,
Shandong, China

Abstract: The purpose of this study was to develop two novel drug delivery systems based on biodegradable docetaxel-lipid-based-nanosuspensions. The first one was poly(ethylene glycol)-modified docetaxel-lipid-based-nanosuspensions (pLNS). It was developed to increase the cycle time of the drug within the body and enhance the accumulation of the drug at the tumor site. The second one was targeted docetaxel-lipid-based-nanosuspensions (tLNS) using folate as the target ligand. The tLNS could target the tumor cells that overexpressed folate receptor (FR). The morphology, particle size, and zeta potential of pLNS and tLNS were characterized, respectively. The in vitro cytotoxicity evaluation of Duopafei®, pLNS, and tLNS were performed in human hepatocellular liver carcinoma HepG2 (FR−) and B16 (FR+) cells, respectively. The in vivo antitumor efficacy and pharmacokinetics, as well as the drug tissue distribution, were evaluated in Kunming mice bearing B16 cells. The particle size of pLNS was 204.2 ± 6.18 nm and tLNS had a mean particle size of 220.6 ± 9.54 nm. Cytotoxicity of tLNS against B16 (FR+) cell lines was superior to pLNS ($P < 0.05$), while there was no significant difference in the half maximum inhibitory concentration values for HepG2 (FR−) cells between pLNS and tLNS. The results of the in vivo antitumor efficacy evaluation showed that tLNS exhibited higher antitumor efficacy by reducing tumor volume ($P < 0.01$) compared with Duopafei and pLNS, respectively. The results of the in vivo biodistribution study indicate that the better antitumor efficacy of tLNS was attributed to the increased accumulation of the drug in the tumor.

Keywords: lipid-based-nanosuspensions, docetaxel, cancer therapy, folate, target drug delivery

Introduction

Recently, nanosuspensions have emerged as a promising strategy for the efficient delivery of poorly soluble drugs. Nanosuspensions can be defined as colloidal dispersions of nanosized drug particles that are produced by a suitable method and stabilized by a suitable stabilizer.[1,2] As nanoparticulate drug delivery systems, nanosuspension particles can be accumulated at the target site either by passive or active targeting mechanisms.[3]

In a previous study,[4] passive docetaxel-lipid-based-nanosuspensions (DTX-LNS) were successfully prepared by the high-pressure homogenization method. Using injectable phospholipids as a stabilizer, DTX-LNS hold the advantages of nanosuspensions and lipid-based-nanocarriers as follows: (1) improved drug dispersibility; (2) enhanced drug solubilization; (3) enhanced drug transmembrane transport capability; (4) increased therapeutic efficacy and reduced toxicity; and (5) appropriate for large-scale production. The aim of this study was to develop long circulating and

Correspondence: Na Zhang
School of Pharmaceutical Sciences,
Shandong University, 44 Wenhua Xi Road,
Jinan 250012, Shandong, China
Tel +86 531 8838 2015
Fax +86 531 8838 2548
Email zhangnancy9@sdu.edu.cn

active targeting LNS based on DTX-LNS by modifying them with functionalized surface coatings.

Enhanced permeation and retention effect is now considered a major mechanism because of their unique biodistribution profile in the tumor tissue. Recent reports demonstrate that surface modification of nanocarriers with poly(ethylene glycol) (PEG) has emerged as a strategy to significantly reduce the rapid mononuclear phagocyte system uptake of nanoparticles and to increase the blood circulation half-life of the drugs; however, they cannot be delivered to specific cells in a target-specific manner.[5–7] To further improve targeting to cancer cells, the most promising strategy involves the use of various targeting moieties or ligands that bind specifically to a receptor that is expressed primarily on malignant cells.[8–10] Moieties or ligands can be attached to the surface of nanocarriers, and thus can deliver the drug specifically into the cancer cell via receptor-mediated endocytosis with minimal accumulation at nonspecific sites. Recently, the receptor for folate (FA) – known as FA receptor (FR) – constitutes a useful targeting site for tumor-specific drug delivery.[11,12] Reasons for this include: (1) FR is overexpressed in many human cancer cells, including malignancies of the ovary, brain, kidney, breast, myeloid cells, and lung;[13] (2) as the stage/grade of the cancer is more advanced, significant upregulation of FR on tumor tissue appears to increase; and (3) FR binding affinity ($K_d = 1 \times 1^{-10}$ M) and the internalization via receptor-mediated endocytosis does not appear to be affected when its ligand is conjugated to nanocarriers via its γ-carboxyl.[14] Thus, FA is an attractive ligand because of its low immunogenicity, ease of modification, and low cost.[15] The small size of FA also allows for good tissue penetration and rapid clearance from receptor negative tissues.[15] As such, FA-based targeting systems present an effective means of selectively delivering therapeutic agents to tumors.[16–18]

To the authors' knowledge, the manufacture of active targeting nanosuspensions on a large scale is difficult. The purpose of this study is to prepare active targeting LNS, which can be targeted to the tumor cells that overexpress FR. On the basis of previous experimental studies, in this study, a PEG-modified DTX-LNS (pLNS) was designed, and then an FA-mediated drug delivery system (targeted DTX-LNS [tLNS]) using synthesized FA-PEG-distearoylphosphatidylethanolamine (FA-PEG-DSPE) conjugate was developed. The morphology, particle size, and zeta potential of pLNS and tLNS were characterized, respectively. The in vitro drug release was assessed using the dialysis bag diffusion technique. The in vitro cytotoxicity studies were done in a murine malignant melanoma cell line (B16), which overexpresses FR (ie, FR-positive [FR+]),[19] and a human hepatoblastoma cell line (HepG2), which is FR-negative (FR−).[20] Finally, the in vivo antitumor efficacy and pharmacokinetics, as well as the drug tissue distribution, were evaluated in Kunming mice bearing B16 cells.

Materials and methods
Materials
Injectable soya lecithin (phosphatidylcholine accounts for 95%, pH 5.0–7.0) was provided by Shanghai Taiwan Pharmaceutical Co, Ltd (Shanghai, China). Duopafei® was provided by Qilu Pharmaceutical Co, Ltd (Jinan, China). DSPE-PEG2000-amine and DSPE-PEG2000-methoxy were purchased by Avanti Polar Lipids Inc (Alabaster, AL). FA was purchased from Sigma-Aldrich Shanghai Trading Co, Ltd (Shanghai, China). Dicyclohexylcarbodiimide, N-hydroxysuccinimide, and dimethyl sulfoxide (DMSO) were obtained from Sinopharm Group Co, Ltd (Shanghai, China). All reagents for high-performance liquid chromatography (HPLC) analysis, including acetonitrile and methanol were of HPLC grade. All the other chemicals and reagents used were of analytical purity grade or higher and obtained commercially.

Animals
The female Kunming mice (weight: 18–22 g, age: 6–8 weeks) were supplied by the Medical Animal Test Center of Shandong University (Jinan, China). The animals were acclimatized for at least 1–2 weeks before experimentation, fed with a standard diet, and allowed water ad libitum. All experiments were carried out in compliance with the Animal Management Rules of the Ministry of Health of the People's Republic of China (document number 55, 2001) and the guidelines for the Care and Use of Laboratory Animals of China Pharmaceutical University.

Synthesis and characterization of DSPE-PEG2000-FA
DSPE-PEG2000-FA was synthesized by a previously described method.[21] Briefly, 13.0 mg folic acid was dissolved in 1 mL DMSO. DSPE-PEG2000-amine (40 mg) and pyridine (250 μL) were added to the reaction solution, followed by 20 mg dicyclohexylcarbodiimide. After the completion of the reaction (about 24 hours at room temperature), the pyridine was removed by rotary evaporation (RE5298; Shanghai Yarong Biochemistry Instrument Factory, Shanghai, China), and then 5 mL water was added to the solution. The solution was dialyzed with a 3500 Da molecular weight cutoff dialysis

bag (Sigma-Aldrich) against 1000 mL 50 mM saline for 1 day and against 1000 mL distilled water for 2 days to remove excess unreacted substrates. The product was lyophilized and the final yield was 40.54 mg (88%). All processes were operated in the dark. Figure 1 depicts the synthesis of DSPE-PEG2000-FA, and the structure of the product was confirmed with ^{1}H nuclear magnetic resonance (Avance™ DPX-300; Bruker BioSpin GmbH, Rheinstetten, Germany). DSPE-PEG2000-FA was also measured – in DMSO-d_6 – using this 400 MHz spectrometer (Avance DPX-300).

Quantitation of FA content

The ultraviolet (UV) method[22] was used to determine the quantitation of FA content. FA (10 mg) was dissolved in 10 mL DMSO, and then the solution was diluted to different concentrations (5–80 µg/mL). They were measured with UV-visible spectrophotometer (UV-2102PCS; UNICO [SHANG-HAI] Instruments Co., Ltd, Shanghai, China) at 365 nm, and the standard curve in the range of 5–80 µg/mL was obtained. The content of conjugated FA was estimated from the UV-visible spectroscopy based on a calibration curve of free FA under the same UV-visible condition assuming an identical molar absorbance for free FA and polymer-conjugated FA.

Preparation of pLNS and tLNS

The DTX-LNS were prepared by high-pressure homogenization and were made with defined molar ratios of lipids. pLNS were made up of soya lecithin/DSPE-PEG2000 94/6 mol% and tLNS were made up of soya lecithin/DSPE-PEG2000/DSPE-PEG2000-FA 94/5.5/0.5 mol%. An appropriate amount of lipid was dissolved in water to obtain the aqueous surfactant solution, which was poured into DTX (0.1% weight/volume) powder and the mixture was sheared under high-speed shearing to obtain drug coarse suspensions. These coarse suspensions were then circulated through a high-pressure homogenizer (Panda 1K NS1001L; Niro Soavi SpA, Parma, Italy) until an equilibrium size was reached.

The freshly prepared pLNS and tLNS were dispensed into glass vials, and mannitol (5% weight/volume) was added to the vials as a lyoprotectant and frozen for 24 hours at −80°C. Those vials were then transferred to a freeze dryer (LGJ0.5; Beijing Four-Ring Scientific Instrument Co, Beijing, China) and dried for 48 hours at −40°C at a pressure of 0.5 mbar to get the lyophilized pLNS and tLNS, respectively.

HPLC analysis of DTX

DTX concentration was measured at 230 nm by HPLC (SPD-10 AVP Shimadzu pump, LC-10AVP Shimadzu UV-visible detector; Shimadzu Corporation, Tokyo, Japan).[4] Samples were chromatographed on a 4.6 × 250 mm reverse phase stainless steel column packed with 5 µm particles (Venusil XBP C18; Bonna-Agela, Tianjin, China) eluted with a mobile phase consisting of acetonitrile/water (55/45 volume/volume) at a flow rate of 1 mL/minute. The column was maintained at room temperature. The samples were properly diluted by
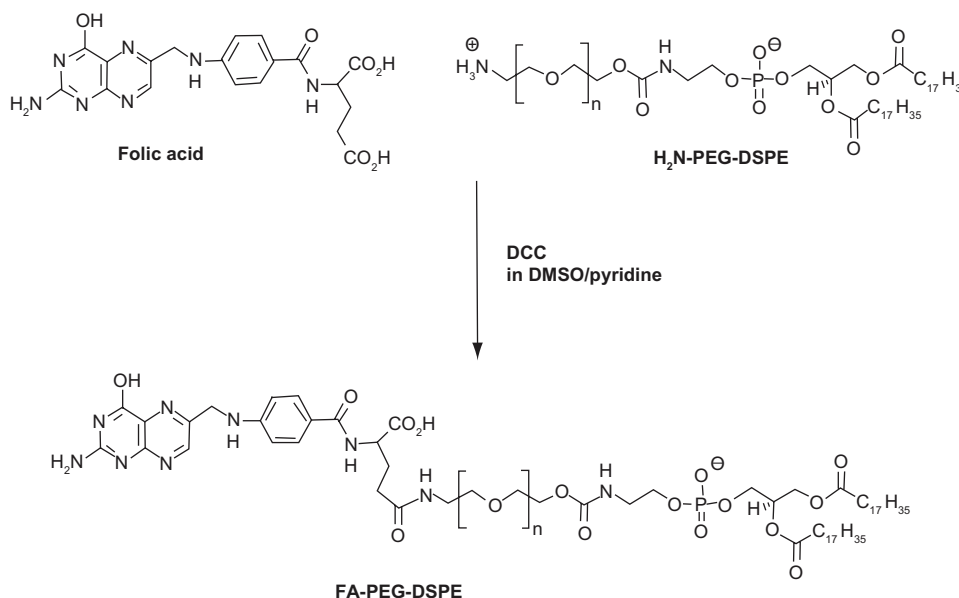

Figure 1 Schematics of the synthetics of distearoylphosphatidylethanolamine-poly(ethylene glycol)2000-folate.
Abbreviations: DCC, dicyclohexylcarbodiimide; DMSO, dimethyl sulfoxide; DPSE, distearoylphosphatidylethanolamine; PEG, poly(ethylene glycol).

methanol and directly injected (20 µL) into the HPLC system without further treatment. The calibration curve of peak area (A) against concentration of DTX (C) was A = 12,684C − 722.76 (r = 0.9998) under the concentration of DTX 1–50 µg/mL; the limit of detection was 0.02 µg/mL.

Stability of pLNS and tLNS

The physical stability of the lyophilized tLNS and pLNS was evaluated at 4°C ± 2°C and 25°C ± 2°C. The changes in particle size and drug content were recorded over a period of 3 months.

In vitro release studies

The in vitro release of DTX from pLNS and tLNS was conducted by dialysis bag diffusion method. Lyophilized pLNS, tLNS, and Duopafei were suspended in 2 mL of deionized water (final DTX concentration 100 µg/mL) and placed into a preswelled dialysis bag with 8–12 kDa molecular weight cutoff. The bag was incubated in 15 mL release medium (0.5% of Tween 80® [Sigma-Aldrich] in phosphate buffered saline, pH 7.4) at 37°C ± 0.5°C under horizontal shaking.[23] At predetermined time points the dialysis bag was taken out and placed into a new container filled with 15 mL fresh medium. The amount of DTX released was determined by the HPLC method described above. Sink condition was maintained throughout the release period. Data obtained in triplicate were analyzed graphically.

In vitro cytotoxicity studies

The cytotoxicity of pLNS and tLNS was tested in HepG2 and B16 cells using a methylthiazol tetrazolium (MTT) assay.[24] Briefly, cells were seeded in a 96-well plate at a density of 4000 viable cells per well and incubated for 24 hours to allow cell attachment. Cells were exposed to a series of doses of Duopafei, blank pLNS, blank tLNS, pLNS, and tLNS, respectively, at 37°C. The range of concentrations of DTX used was 0.01, 0.1, 1, 2, and 10 µM. After 48 hours of incubation, 20 µL of MTT (5 mg/mL) was added to each well. Four hours later, DMSO (200 µL per well) was added to dissolve the contents in the plate, and the absorbance of the obtained DMSO solution was measured at 570 nm and 630 nm by a microplate reader (FL600™; BioTek Instruments, Winooski, VT). Nontreated cells were taken as control with 100% viability, and cells without addition of MTT were used as blanks to calibrate the spectrophotometer to zero absorbance.[25]

In vivo antitumor efficacy

Kunming mice implanted with B16 cells were used to qualify the efficacy of DTX-LNS intravenously.[4] The mice were subcutaneously injected at the right axillary space with 0.1 mL of cell suspension containing 5×10^4 B16 cells.[26] Treatments started 8–10 days after implantation in mice with a tumor volume of ~100 mm³. The mice were randomly assigned to one of the six treatment groups. Each group of mice was treated every 3 days with the different formulations as described in the following: 1) pLNS (DTX concentration of 20 mg/kg, diluted in physiological saline); 2) tLNS (DTX concentration of 20 mg/kg, diluted in physiological saline); 3) Duopafei (dosage of 20 mg/kg, diluted in physiological saline); 4) normal saline (NS); 5) blank pLNS; and 6) blank tLNS.

All mice were labeled, and tumors were measured every other day with calipers during the experiment period. The tumor volume (V) was calculated by the formula: $V = (W^2 \times L)/2$, where W is the tumor measurement at the widest point and L is the tumor dimension at the longest point. Each animal was weighed at the time of treatment so that dosages could be adjusted to achieve the mg/kg amounts reported. The animals were also weighed every other day during the experiment period and monitored as an index of systemic toxicity.[27] After 21 days, the animals were killed, and the tumor mass was harvested, weighed, and photographed. The tumor inhibition ratio (TIR) could be defined as follows: TIR (%) = ([$W_c − W_t]/W_c$) × 100, where W_c and W_t stand for the average tumor weight for the control group and treatment group, respectively.[26]

Pharmacokinetics and tissue distribution

The tumor-bearing mice were selected randomly and equally divided into three groups as subjects. Three formulations – Duopafei, pLNS, and tLNS – were administered to the three groups, respectively, at a 60 mg/kg dose level via the tail vein. Blood samples were taken from the retroorbital plexus at predetermined time points: Duopafei (5, 15, 30, and 45 minutes; 1, 2, 3, 4, 5, 6, 7, and 8 hours); pLNS and tLNS (5, 15, 30, and 45 minutes; 1, 2, 4, 6, 8, 10, and 12 hours). The mice were then euthanized by cervical dislocation, and the tumor, heart, liver, spleen, lung, and kidney were collected, washed, weighed, and homogenized (T 10 Ultra-Turrax®; IKA®-Werke GmbH, Staufen, Germany) in 1 mL of physiological saline. After collection, both plasma and tissue samples were stored at −20°C until further analysis.

Serum and tissue sample analysis

The plasma samples were extracted as previously reported. DTX plasma concentrations were determined as follows. Briefly, 200 µL of plasma samples were extracted by vortex-mixing (VORTEX-5; Jiangsu Nanjing Zhituo Instrument

Factory, Jiangsu, China) the samples for 30 seconds after adding 250 μL methanol and 250 μL acetonitrile. The mixture was then centrifuged (Anke TGL-16G-A; Shanghai Anting Scientific Instrument Co., Ltd, Shanghai, China) for 15 minutes at 15,000 rpm, and the supernatant was transferred, filtered, and injected into the HPLC system.

The tissue sample was weighed accurately and homogenized using a tissue homogenizer after addition of 1 mL physiologic saline. Tissue homogenates (200 μL) were processed similarly to the above disposal methods for plasma samples and analyzed by HPLC.

Pharmacokinetics and statistical analysis

The main pharmacokinetic parameters were calculated by the statistical moment method using Debris Assessment Software version 2.0 (NASA Orbital Debris Program Office, Houston, TX). The area under the plasma concentration-time profiles, distribution, elimination half-life, mean residence time, and total plasma clearance were calculated. All studies were repeated at least three times and measured at least in triplicate. Results were reported as mean ± standard deviation. Statistical significance was analyzed using Student's t-test. Differences between experimental groups were considered significant when $P < 0.05$.

Results and discussion
Characterization of DSPE-PEG2000-FA

The final product was a yellow dry powder (molecular weight 3231 Da). [1]H nuclear magnetic resonance spectra of DSPE-PEG2000-FA (Figure 2) was: δ = 8.64 (s, 1H, C7-H), 7.65 (d, 2′, 6′-H, 2H), 6.67 (d, 3′, 5′-H, 2H), 5.07 (m, PO_4CH_2CH, 1H), 4.51 (d, 9-CH_2N, 2H), 4.31 (m, α-CH, 1H), 4.27 (dd, cis-PO_4CH_2CH, 1H), 4.11 (dd, trans-PO_4CH_2CH, 1H), 4.02 (t, CH_2OCONH, 2H), 3.54 (s, PEG, 180H), 3.1 (m, CH_2CH_2N, 4H), 2.2–2.5 (overlapping $2 \times$ t, CH_2CH_2CO and m, CH_2 of Glu, 8H), 1.49 (m, CH_2CH_2CO, 4H), 1.22 (s, CH_2, 56H), and 0.84 (t, CH_3, 6H). These results are in agreement with previously published studies, confirming the successful synthesis of the DSPE-PEG2000-FA conjugate.[21,28]

Determination of FA content

FA showed three maximum absorption peaks at 256, 283, and 365 nm.[22] The UV cutoff of DMSO was quite high at 268 nm; in addition, the intensity of the absorption peak decreased at 283 nm. Therefore, 365 nm was used as the determinate wavelength.

When the conjugate concentration was 0.08 mg/mL, the absorbency was 0.014, thus the content of FA determined in the polymer was 0.256 mmol/g (82.58% of the theoretical value). Therefore, the FA-modified rate of DSPE-PEG2000-FA polymer was more than 80%.

Design, preparation, and characterization of pLNS and tLNS

In the present study, two biodegradable DTX-LNS were prepared. The first system was pLNS, which was developed to increase the cycle time of the drug within the body and enhance the accumulation of the drug at the tumor site. The second one was tLNS using FA as the target ligand. tLNS can target the tumor cells that overexpress FR, and can be successfully employed for large-scale production.
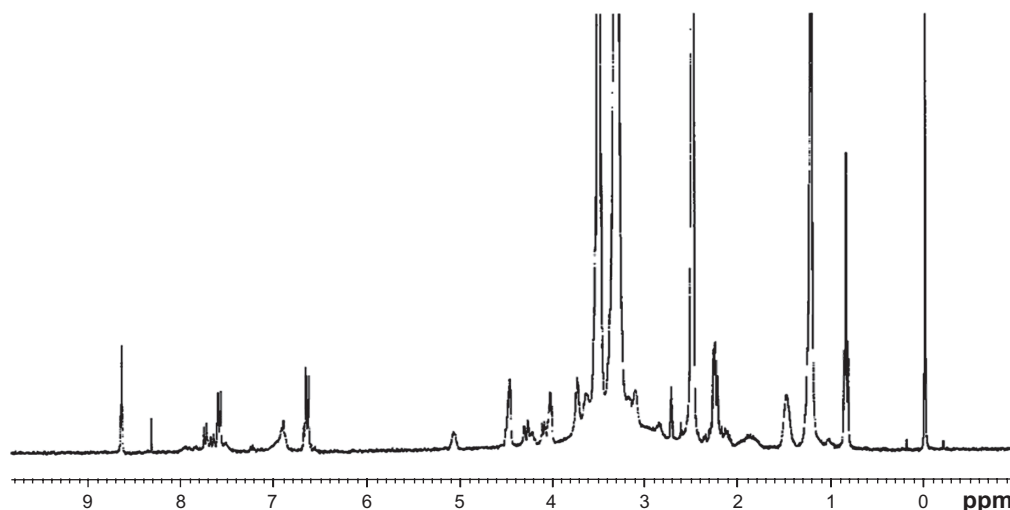

Figure 2 ^{1}H nuclear magnetic resonance spectra of synthesized distearoylphosphatidylethanolamine-poly(ethylene glycol)2000-folate in dimethyl sulfoxide-d$_6$.
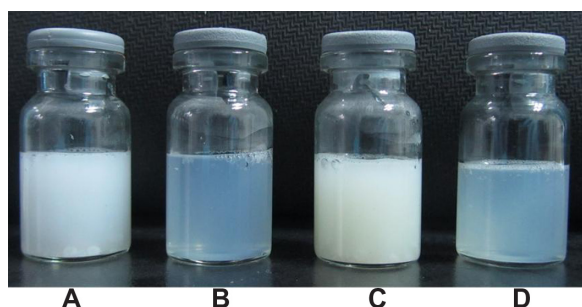**Abbreviation:** ppm, parts per millon.

Figure 3 Photographs of (**A**) coarse poly(ethylene glycol)-mediated docetaxel-lipid-based-nanosuspension; (**B**) poly(ethylene glycol)-mediated docetaxel-lipid-based-nanosuspension; (**C**) coarse targeted docetaxel-lipid-based-nanosuspension; and (**D**) targeted docetaxel-lipid-based-nanosuspension.

Photographs of coarse pLNS, pLNS, coarse tLNS, and tLNS are shown in Figure 3. Adkins et al reported that an appearance of nanoparticles with particle size ranging from 50–200 nm shows transparent liquid.[29,30] The transparent pLNS and tLNS obtained in the present study appear to have micronized completely. The transmission electron micrograph of the freshly prepared pLNS and tLNS are shown in Figure 4. The particle size of pLNS was 204.2 ± 6.18 nm (polydispersivity index 0.192 ± 0.010) with a zeta potential of −33.83 ± 0.35 mV. The particle size of tLNS was 220.6 ± 9.54 nm (polydispersivity index 0.173 ± 0.031) with a zeta potential of −27.80 ± 0.77 mV. The freeze-dried pLNS and tLNS were spherical or ellipsoidal in shape (Figure 5). The mean particle size of the freeze-dried pLNS and tLNS was 228.8 ± 8.05 nm (polydispersivity index 0.197 ± 0.026) and 241.3 ± 4.61 nm (polydispersivity index 0.191 ± 0.017), respectively. The zeta potentials were −32.69 ± 0.43 mV and −27.45 ± 0.28 mV, respectively.
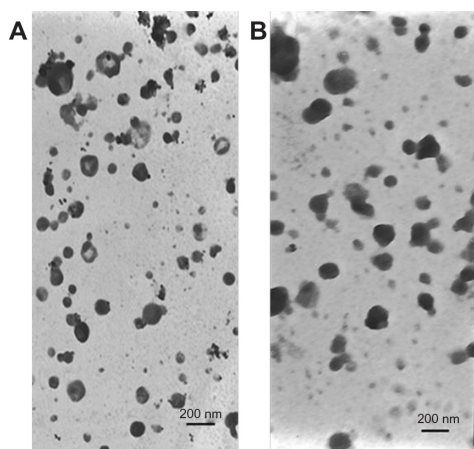

Figure 4 Transmission electron photomicrographs of freshly prepared (**A**) poly(ethylene glycol)-mediated docetaxel-lipid-based-nanosuspension; and (**B**) targeted docetaxel-lipid-based-nanosuspension.
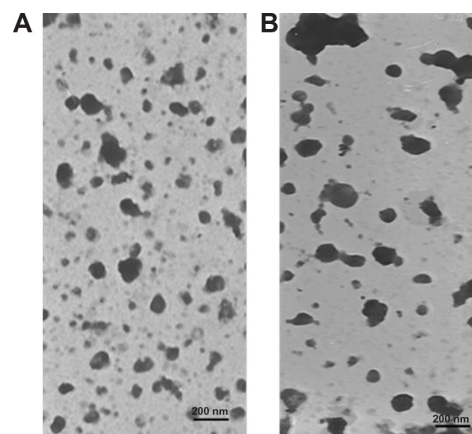

Figure 5 Transmission electron photomicrographs of freeze dried (**A**) poly(ethylene glycol)-mediated docetaxel-lipid-based-nanosuspension; and (**B**) targeted docetaxel-lipid-based-nanosuspension.

Stability of pLNS and tLNS

The physical stability of the lyophilized pLNS and tLNS was evaluated over 3 months at 4°C ± 2°C and 25°C ± 2°C. During this storage period, the particle size did not significantly change, and more than 99% of DTX remained in the nanosuspensions, indicating that the lyophilized product has a shelf-life of at least 3 months.

In vitro drug release

The release experiment was conducted under sink conditions and the release profiles were obtained by representing the percentage of free drug from LNS. Both the release behavior of DTX from pLNS and tLNS followed the first-order kinetics equation, and can be expressed as follows: pLNS, $\ln(100 - Q) = -0.084\,t + 4.588$ (r = 0.9985); tLNS, $\ln(100 - Q) = -0.066\,t + 4.567$ (r = 0.9980), where Q is the amount released and t is time. The release profiles of pLNS and tLNS are shown in Figure 6. No differences were seen in the release behavior between pLNS and tLNS, and the cumulative amount of drug released reached 100% within 36 hours. The release behavior of DTX from Duopafei also followed the first-order kinetics equation and approximately 100% of DTX in Duopafei was released within 24 hours. This phenomenon could be attributed to a decrease in the mean nanoparticle size, leading to an increase in the dissolution velocity. Besides, an increase in drug solubility may be mainly due to the drug nanosuspensions, which have a higher surface area and are sufficiently exposed to the aqueous dispersion medium, thus leading to increased saturation solubility.[1,31,32]

In vitro cytotoxicity

The LNS were evaluated for in vitro cytotoxicity in FR+ B16 and FR− HepG2 cells by MTT assay. The half maxi-
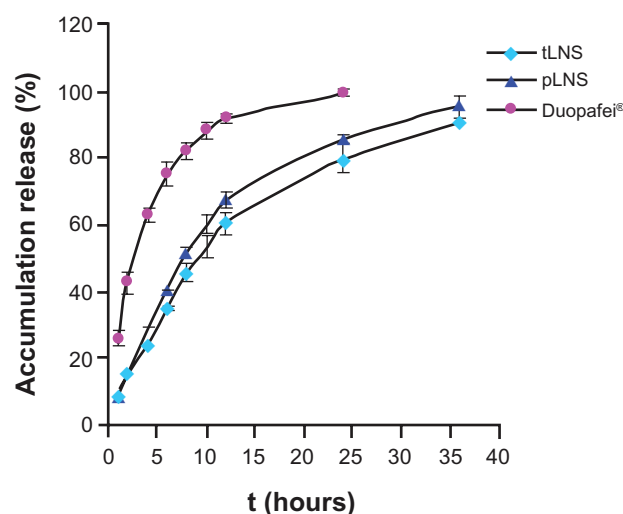
Figure 6 In vitro release profile of docetaxel from poly(ethylene glycol)-mediated docetaxel-lipid-based-nanosuspension, targeted docetaxel-lipid-based-nanosuspension, and Duopafei® in phosphate buffered saline (0.5% of Tween 80® in phosphate buffered saline, pH 7.4) at 37°C ± 0.5°C (n = 3).
Abbreviations: pLNS, poly(ethylene glycol)-mediated docetaxel-lipid-based-nanosuspension; t, time; tLNS, targeted docetaxel-lipid-based-nanosuspension.

mal inhibitory concentration of Duopafei, pLNS, and tLNS for HepG2 and B16 (n = 3) are presented in Table 1. Both Duopafei and LNS formulations exhibited clear dose-dependent cytotoxicity against these cell lines with the concentration of loaded DTX increasing from 0.01 µM to 10 µM (Figure 7). However, blank pLNS and blank tLNS had no effect on cell viability and showed similar results to the nontreated cells ($P > 0.5$). That might be because the main composition of blank pLNS and blank tLNS was phospholipid material, which is a good biocompatible material that can be totally metabolized and nontoxic to cells. On the other hand, there were statistically significant differences in the half maximal inhibitory concentration values of pLNS and Duopafei, implying that pLNS shows higher cytotoxicity against these two cells. The possible mechanism underlying the enhanced efficacy of DTX against tumor cells may include the enhanced intracellular drug accumulation by nanoparticle uptake.[33]

Compared to pLNS, tLNS showed a slightly higher anti-tumor effect in the FR+ B16 cells. In contrast, no therapeutic advantageous effect on cytotoxicity was observed in the FR− HepG2 cell line. These results are in accordance with previous studies in which superior cytotoxicity of FR−targeted nanoparticles over nontargeted nanoparticles was observed in the FR+ cells, but not in the FR− HepG2 cells.[34] According to these results and previous studies,[34,35] it can be speculated that tLNS was able to selectively deliver drugs to FR+ cancer cells, and FA might serve as a targeting ligand to induce internalization by target cells. Detailed studies on the mechanism of internalization are currently being investigated.

In vivo therapeutic experiment

Antitumor activity was evaluated using B16 tumor-bearing mice as a model. According to previous studies,[36–38] statistically significant change in tumor volume is an important indicator for evaluating antitumor efficacy of the different therapy regimens and can be used to define the pharmacokinetics of the different formulations. Figure 8A depicts the change in tumor volume and Figure 8B depicts the excised tumor mass weights. The obvious tumor regression was observed in mice treated with Duopafei, pLNS, and tLNS. It was found that the antitumor effect in the pLNS and tLNS groups was much stronger than in the Duopafei group ($P < 0.01$), and the tumor volumes of the tLNS group were smaller than those treated with pLNS at the same dose ($P < 0.05$). At the end of the test, tumor volumes in mice treated with tLNS were 0.42 ± 0.14 cm^3, which was significantly smaller than the value of 1.49 ± 0.20 cm^3 for the Duopafei group ($P < 0.01$). Significant differences in tumor weights were also observed between the Duopafei group and the groups receiving pLNS and tLNS ($P < 0.01$). To some degree, the statistical significance can reflect the biological significance of the formulations. So, the results indicate that the antitumor effect of pLNS and tLNS on experimental animals was much stronger than that of Duopafei, while no antitumor effect was observed in the NS, blank pLNS, and blank tLNS groups. As shown in Figure 8C, these typical photographs of excised sarcomas from the tested groups provide a direct visual representation of the tumor suppression effect.

Table 1 The half maximal inhibitory concentration of HepG2 and B16 cells incubated with Duopafei®, poly(ethylene glycol)-mediated docetaxel-lipid-based-nanosuspension, targeted docetaxel-lipid-based-nanosuspension, blank poly(ethylene glycol)-mediated docetaxel-lipid-based-nanosuspension, and blank targeted docetaxel-lipid-based-nanosuspension at 48 hours

Cell line	Duopafei	pLNS	tLNS	Blank pLNS	Blank tLNS
B16	1.03 ± 0.15	0.70 ± 0.06**	0.43 ± 0.05##	26.18 ± 2.75	30.79 ± 1.43
HepG2	1.08 ± 0.06	0.65 ± 0.05**	0.69 ± 0.07	24.80 ± 0.67	30.45 ± 1.44

Notes: The range of concentrations of docetaxel used was from 0.01–10 µM (n = 3). Data are presented as mean ± standard deviation; ##$P < 0.01$ versus the poly(ethylene glycol)-mediated docetaxel-lipid-based-nanosuspension group; **$P < 0.01$ versus the Duopafei group.
Abbreviations: pLNS, poly(ethylene glycol)-mediated docetaxel-lipid-based-nanosuspension; tLNS, targeted docetaxel-lipid-based-nanosuspension.
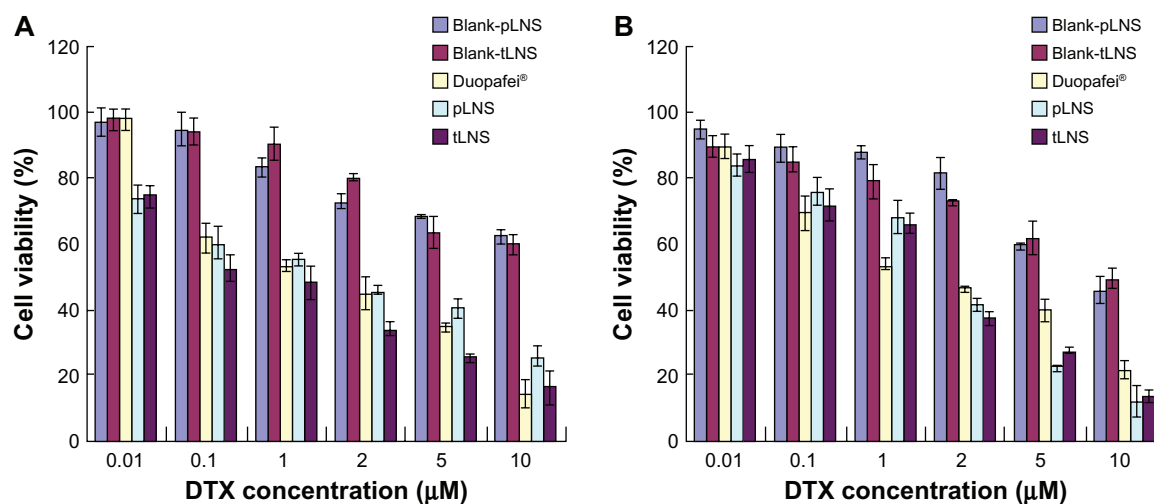
Figure 7 Cytotoxic effects of blank poly(ethylene glycol)-mediated docetaxel-lipid-based-nanosuspension, blank targeted docetaxel-lipid-based-nanosuspension, Duopafei®, poly(ethylene glycol)-mediated docetaxel-lipid-based-nanosuspension, and targeted docetaxel-lipid-based-nanosuspension against (**A**) B16 and (**B**) HepG2 cells.
Note: Data represent mean ± standard deviation (n = 3).
Abbreviations: DTX, docetaxel; pLNS, poly(ethylene glycol)-mediated docetaxel-lipid-based-nanosuspension; tLNS, targeted docetaxel-lipid-based-nanosuspension.
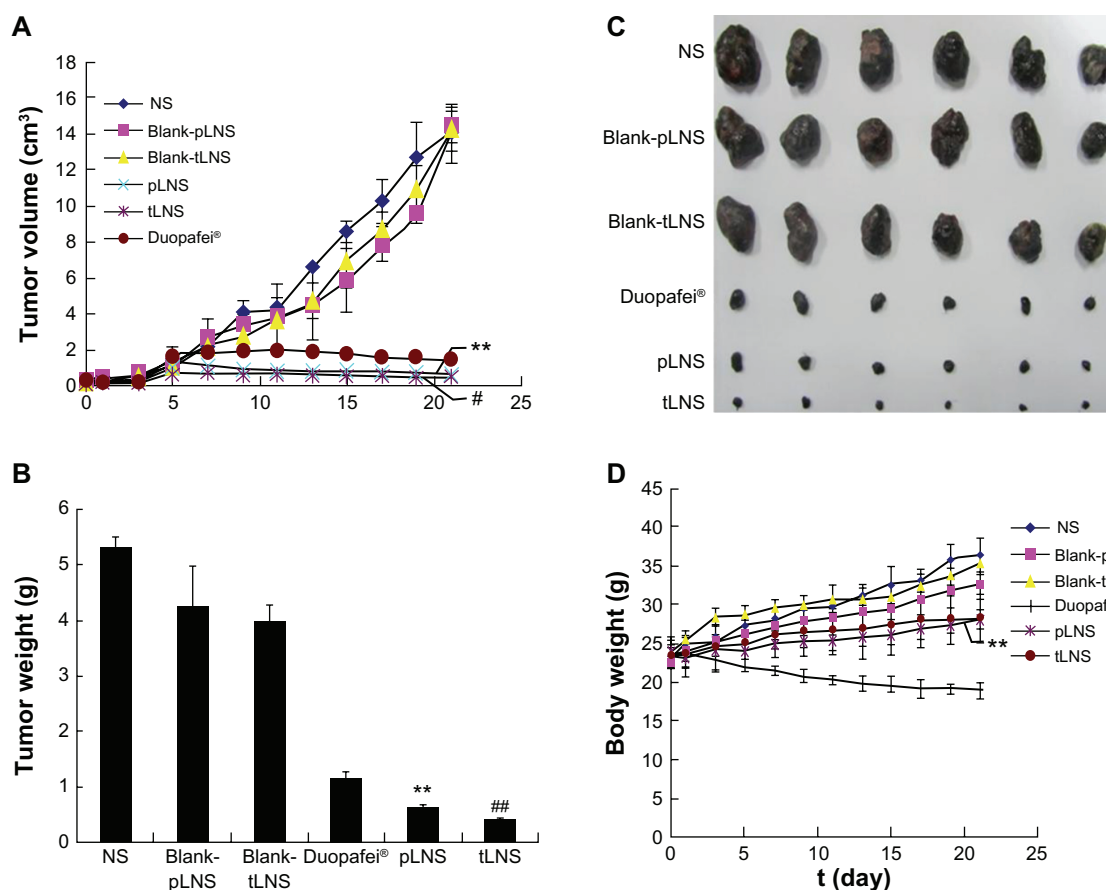

Figure 8 Antitumor effects of poly(ethylene glycol)-mediated docetaxel-lipid-based-nanosuspension, targeted docetaxel-lipid-based-nanosuspension, Duopafei®, blank poly(ethylene glycol)-mediated docetaxel-lipid-based-nanosuspension, blank targeted docetaxel-lipid-based-nanosuspension, and NS on B16 tumor-bearing mice after intravenous administration. Data represent mean ± standard deviation (n = 6). (**A**) Tumor volume; (**B**) tumor weight; (**C**) photographs of tumors excised on day 21; and (**D**) body weight change.
Notes: **$P < 0.01$ versus the Duopafei group; #$P < 0.05$ versus the poly(ethylene glycol)-mediated docetaxel-lipid-based-nanosuspension group; ##$P < 0.01$ versus the poly(ethylene glycol)-mediated docetaxel-lipid-based-nanosuspension group.
Abbreviations: pLNS, poly(ethylene glycol)-mediated docetaxel-lipid-based-nanosuspension; t, time; tLNS, targeted docetaxel-lipid-based-nanosuspension.

The tumor inhibition rates of the pLNS, tLNS, and Duopafei groups compared with the NS group are listed in Table 2. The pLNS group showed a significantly higher tumor inhibition rate ($87.93\% \pm 2.55\%$) than Duopafei ($78.44\% \pm 5.16\%$) ($P < 0.01$). The tLNS group showed a superior tumor inhibition rate ($92.09\% \pm 2.72\%$) to pLNS ($87.93\% \pm 2.55\%$) ($P < 0.01$).

These findings indicate that the high antitumor activity of tLNS was achieved, which could be attributed to the PEG-modified nanoparticles considerably prolonging the drug's half-life in the body, the increased accumulation of the drug at the tumor site, and, ultimately, the ability to reach high levels in the tumor due to the enhanced permeation and retention effect.[39] The antitumor activity of pLNS was also improved by the enhanced permeation and retention effect. tLNS can be taken up by FR-mediated endocytosis to exert its pharmacological effect. This is because once an FA-modified nanoparticle arrives at an FR+ tumor cell, FA will not only increase retention of the nanoparticle in the tumor mass but also facilitate uptake of the particle by FR-mediated endocytosis.[40] Detailed studies on the mechanism of ligand–receptor interactions are currently being investigated.

Figure 8D depicts the variation of the relative body weights of the mice. These results suggest that the mice experienced a large weight increase from the initial day of administration to the end of the experiment. These increases were 56.89%, 44.40%, 48.64%, 18.89%, and 22.07% for NS, blank pLNS, blank tLNS, pLNS, and tLNS, respectively. However, the Duopafei group experienced a slight weight loss ($<10\%$), which was significant compared to that induced by the two DTX-loaded LNS groups ($P < 0.01$). The analysis of body weight variations could be partially used to define the adverse effects of the different therapy regiments.[37] Therefore, pLNS and tLNS generated less toxicity to mice than Duopafei when

administered intravenously under the present experiment condition, which will facilitate its future clinical application. Moreover, it was observed that the mice of the Duopafei group were in a weak state and moved slowly; three of these mice died during the experiment, whereas no obvious alteration was observed in the pLNS and tLNS group.

Overall, these results indicate that tLNS and pLNS showed higher efficacy and much lower side effects in B16 tumor-bearing mice compared with Duopafei, and tLNS showed superior antitumor efficacy to pLNS.

Pharmacokinetic studies

The standard curves with DTX concentrations ranging from $0.5-50\ \mu g/mL$ exhibited good linearity, and correlation coefficients over this concentration range were 0.9994–0.9999 for plasma and all measured organs.

The plasma concentration-time profiles of DTX after intravenous administration of the three formulations in mice is shown in Figure 9. The corresponding pharmacokinetic parameters are presented in Table 3. There was no statistical significant difference in DTX serum concentration between pLNS and tLNS. The pharmacokinetic profiles for DTX showed significant differences for pLNS and tLNS versus Duopafei. After injection of pLNS and tLNS, the DTX serum concentration was still measurable after 12 hours, while it was no longer detectable after 8 hours for the Duopafei group. As shown in Table 4, compared to Duopafei, the area under the plasma concentration-time profiles following intravenous administration of tLNS and pLNS significantly increased by about 1.59 and 1.66 times, respectively ($P < 0.01$), clearance significantly decreased ($P < 0.01$), and the mean residence time was significantly prolonged by about 2.40 and 2.41 times, respectively ($P < 0.05$). These results indicate that the plasma pharmacokinetics of DTX given in these

Table 2 The tumor inhibition ratio of the Duopafei®, poly(ethylene glycol)-mediated docetaxel-lipid-based-nanosuspension, and targeted docetaxel-lipid-based-nanosuspension groups

Group	Dose (mg/kg)	Number of animals (start/end)	Average tumor weight (g)	TIR (100%)	P
NS	–	10/10	5.31 ± 0.19	–	–
Blank pLNS	–	10/10	4.24 ± 0.73	–	–
Blank tLNS	–	10/10	3.97 ± 0.30	–	–
Duopafei	20	10/7	1.15 ± 0.12	78.44 ± 5.16	$<0.01^{\$\$}$
pLNS	20	10/10	0.64 ± 0.04	87.93 ± 2.55	$<0.01^{**}$
tLNS	20	10/10	0.42 ± 0.02	92.09 ± 2.72	$<0.01^{\#\#}$

Notes: $^{\$\$}P < 0.01$ versus the NS group; $^{**}P < 0.01$ versus the Duopafei group; $^{\#\#}P < 0.01$ versus the poly(ethylene glycol)-mediated docetaxel-lipid-based-nanosuspension group.
Abbreviations: NS, normal saline; pLNS, poly(ethylene glycol)-mediated docetaxel-lipid-based-nanosuspension; TIR, tumor inhibition rate; tLNS, targeted docetaxel-lipid-based-nanosuspension.
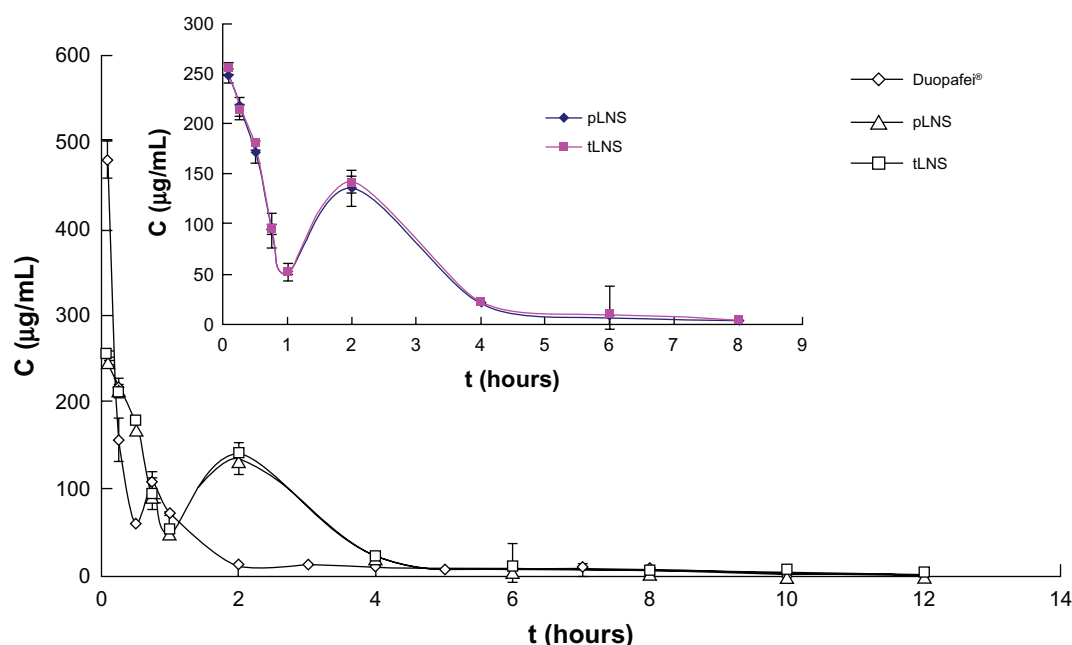
Figure 9 Mean plasma concentration of docetaxel after intravenous administration of Duopafei®, poly(ethylene glycol)-mediated docetaxel-lipid-based-nanosuspension, and targeted docetaxel-lipid-based-nanosuspension.
Note: Data represent mean ± standard deviation (n = 5).
Abbreviations: C, mean concentration; pLNS, poly(ethylene glycol)-mediated docetaxel-lipid-based-nanosuspension; t, time; tLNS, targeted docetaxel-lipid-based-nanosuspension.

two formulations were different from Duopafei. This effect may be due to the lipophilic part of DSPE-PEG2000 merged with the core of the nanosuspension nanoparticles, therefore allowing the hydrophilic PEG chains to swing on the surface of the nanoparticles.[41] It has been reported that PEG-modified nanoparticles can prevent macrophage uptake and achieve a prolonged blood circulation effect to some degree.[42]

Table 3 Plasma pharmacokinetic parameters after intravenous injection of Duopafei®, poly(ethylene glycol)-mediated docetaxel-lipid-based-nanosuspension, and targeted docetaxel-lipid-based-nanosuspension at a dose of 60 mg/kg of docetaxel (n = 5)

Pharmacokinetic parameters	Formulations		
	Duopafei	**pLNS**	**tLNS**
C_{max} (µg/mL)	481.62 ± 13.23	217.92 ± 10.54	213.45 ± 13.16
$T_{1/2\alpha}$ (hours)	0.31 ± 0.06	0.230 ± 0.19	0.230 ± 0.08
$T_{1/2\beta}$ (hours)	1.78 ± 0.11	3.68 ± 0.23**	3.70 ± 0.17**
T_{max} (hours)	0.083	0.083	0.083
$AUC_{0-\infty}$ (mg/L/hour)	308.42 ± 20.23	489.65 ± 11.19**	511.30 ± 19.81**
MRT (hours)	1.76 ± 0.15	4.229 ± 0.17*	4.230 ± 0.67*
CL (L/hour/kg)	0.195	0.100**	0.097**

Notes: Data are presented as mean ± standard deviation. *$P < 0.05$ versus the Duopafei group; **$P < 0.01$ versus the Duopafei group.
Abbreviations: $AUC_{0-\infty}$, area under the plasma concentration-time profiles; CL, total plasma clearance; C_{max}, maximum concentration; MRT, mean residence time; pLNS, poly(ethylene glycol)-mediated docetaxel-lipid-based-nanosuspension; tLNS, targeted docetaxel-lipid-based-nanosuspension; $T_{1/2\alpha}$, distribution; $T_{1/2\beta}$, elimination half-life; T_{max}, time to maximum concentration.

Tissue distribution of pLNS and tLNS

The results of the in vitro cytotoxicity assays for DTX formulations suggest that tLNS has a better potential for tumor targeting. Therefore, the tissue distribution of tLNS was focused on.

The tissue DTX concentrations versus time after intravenous administration of Duopafei, pLNS, and tLNS are shown in Figure 10. Tissues (liver, spleen, and lung) showed significantly higher DTX concentrations in the pLNS and tLNS groups compared with Duopafei ($P < 0.01$), while both

Table 4 Targeting disposition of docetaxel after intravenous administration of Duopafei®, poly(ethylene glycol)-mediated docetaxel-lipid-based-nanosuspension, and targeted docetaxel-lipid-based-nanosuspension to mice at a dose of 60 mg/kg of docetaxel (n = 5)

Tissue	Duopafei	pLNS			tLNS		
	T_e (%)	T_e (%)	r_e	C_e	T_e (%)	r_e	C_e
Heart	24.03	4.92	0.97	0.51	4.84	0.96	0.49
Liver	8.58	32.50	17.86	2.80	30.96	17.14	2.79
Spleen	18.91	39.31	9.80	2.40	39.70	9.97	2.32
Lung	19.23	13.19	3.23	1.79	13.63	3.37	1.77
Kidney	22.31	4.40	0.93	0.41	4.47	0.95	0.38
Tumor	5.22	5.67	5.22	1.02	6.40	5.92	1.17

Abbreviations: C_e, maximum concentration; pLNS, poly(ethylene glycol)-mediated docetaxel-lipid-based-nanosuspension; r_e, relative efficiency; T_e, targeting efficiency; tLNS, targeted docetaxel-lipid-based-nanosuspension.

of these two formulations decreased the DTX concentrations in the heart and kidney, which would be expected to reduce the side effects of the drug. At 8 hours after dosing, the drug concentration from tLNS remained higher in comparison with pLNS and far superior to Duopafei ($P < 0.01$) (Table 4 and Figure 11).

The overall targeting efficiency of pLNS was 1.09 times better than that of Duopafei (5.22% versus 5.67%, respectively), the relative efficiency was 5.22, and the maximum concentration in the tumor was 1.02. The targeting efficiency of tLNS was 1.13 times better than that of pLNS (5.67% versus 6.40%, respectively), the relative efficiency was 5.92, and the maximum concentration in the tumor was 1.17, which indicates that tLNS could increase the accumulation of DTX within tumors and achieve great targeting ability.

The mechanisms of targeting nanocarriers to cancer are generally categorized as either passive or active targeting strategies.[43] The active targeting strategy involves the use of a ligand that binds specifically to a receptor that is expressed primarily on malignant cells. It can be exploited to carry the nonselective drugs specifically into the cancer cell and improve the pharmacokinetics of the drugs. Thanks to the passive or active targeting strategies, in this study both pLNS and tLNS provided biodistribution and pharmacokinetic advantages compared to Duopafei.

The clearance behavior and tissue distribution of intravenously injected particulate drug carriers are greatly influenced by their size, surface features, and opsonization.[5] Therefore, the size of the nanosuspensions was controlled and the surface properties were changed to avoid opsonization and improve their distribution to tumors. For pLNS, the presence of a hydrophilic chain PEG swing on the surface of the nanoparticles could lead to a longer retention time in the body and passive targeting potential to the tumor mass. For tLNS, nanosuspension particles could further enhance the targeting to FR+ tumor cells by active targeting. Once an FA-linked nanoparticle arrives at an FR+ tumor cell (eg, B16 cells),
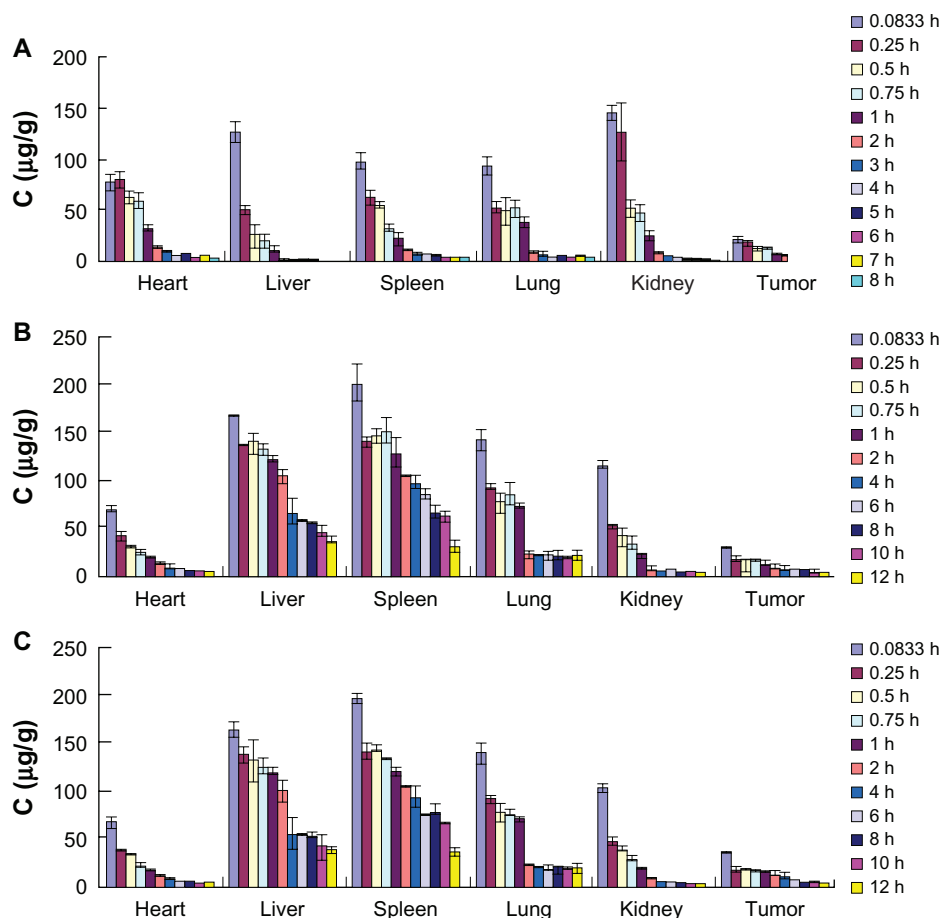

Figure 10 The distribution of docetaxel in mice organs at different time points after intravenous administration of (**A**) Duopafei®; (**B**) poly(ethylene glycol)-mediated docetaxel-lipid-based-nanosuspension; and (**C**) targeted docetaxel-lipid-based-nanosuspension.
Note: Data represent mean ± standard deviation (n = 5).
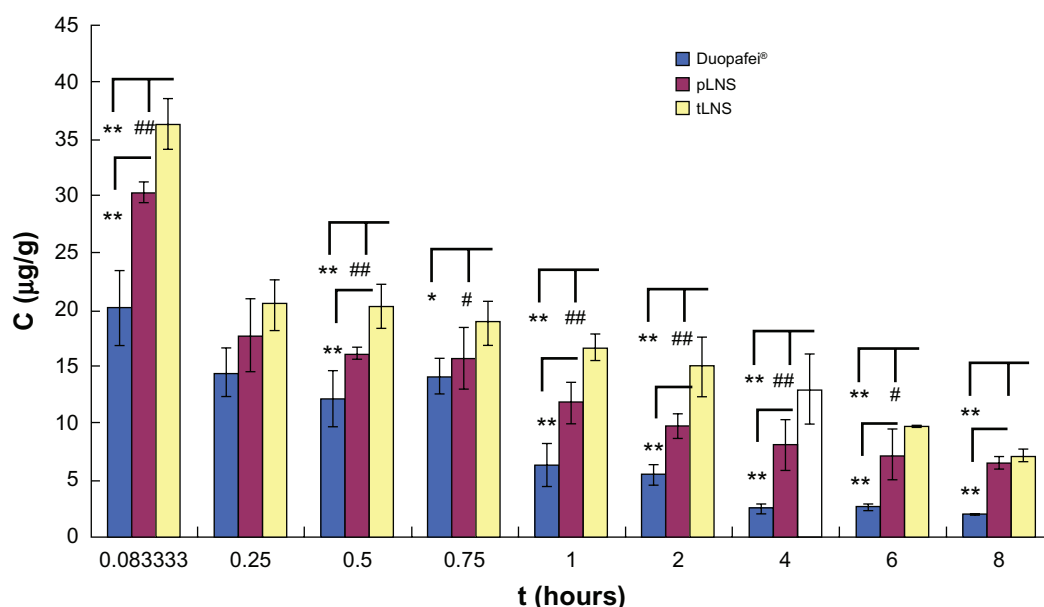**Abbreviations:** C, concentration; h, hours.

Figure 11 Distribution of docetaxel in tumor tissues of mice after intravenous administration of Duopafei®, poly(ethylene glycol)-mediated docetaxel-lipid-based-nanosuspension, and targeted docetaxel-lipid-based-nanosuspension.
Notes: Data represent mean ± standard deviation (n = 5). *$P < 0.05$ versus the Duopafei group; **$P < 0.01$ versus the Duopafei group; #$P < 0.05$ versus the poly(ethylene glycol)-mediated docetaxel-lipid-based-nanosuspension group; ##$P < 0.01$ versus the poly(ethylene glycol)-mediated docetaxel-lipid-based-nanosuspension group.
Abbreviations: C, concentration; pLNS, poly(ethylene glycol)-mediated docetaxel-lipid-based-nanosuspension; t, time; tLNS, targeted docetaxel-lipid-based-nanosuspension.

ligation of the particle to FA could enhance the therapeutic efficacy of the loaded drug, since FA would increase retention of the nanoparticle in the tumor mass and facilitate uptake of the particle by FR-mediated endocytosis.[40]

Tumor accumulation for the tLNS group was significantly greater than the pLNS group and far superior to the Duopafei group ($P < 0.01$). tLNS holds tremendous potential as a carrier for drugs to target cancer cells.

Conclusion

In the present study, it was demonstrated that the FA-modified tLNS has several advantages that are necessary in cancer therapy: (1) maximal accumulation and penetration into the tumor site via FA, which could target deliver the nanosuspensions to cancer cells overexpressing FR; (2) less accumulation in nontargeted tissues; (3) less toxicity to normal organs and tissues compared with Duopafei; and (4) higher efficacy and lower side effects compared with Duopafei. In addition, tLNS could be successfully prepared by the high-pressure homogenization method. They were easy to manufacture and the production processes described earlier could easily be scaled up for commercial production.[1] This progress is vital to the application of target therapy strategies.

Above all, the novel formulation could be a promising solution for the delivery of antitumor drugs to cancerous

tissue. In future work, the authors will need stricter research to further evaluate the in vivo antitumor effect and toxicity of LNS. The precise transfer mechanism of tLNS and, ultimately, the feasibility and advantages of clinical applications will also be focused on.

Acknowledgments

Disclosure

The authors report no conflicts of interest in this work.

References
1. Patravale VB, Date AA, Kulkarni RM. Nanosuspensions: a promising drug delivery strategy. *J Pharm Pharmacol*. 2004;56(7):827–840.
2. Ali HS, York P, Blagden N. Preparation of hydrocortisone nanosuspension through a bottom-up nanoprecipitation technique using microfluidic reactors. *Int J Pharm*. 2009;375(1–2):107–113.
3. Maeda H, Matsumura Y. Tumoritropic and lymphotropic principles of macromolecular drugs. *Crit Rev Ther Drug Carrier Syst*. 1989;6(3):193–210.
4. Wang L, Liu Z, Liu D, Liu C, Juan Z, Zhang N. Docetaxel-loaded-lipid-based-nanosuspensions (DTX-LNS): preparation, pharmacokinetics, tissue distribution and antitumor activity. *Int J Pharm*. 2011;413(1–2):194–201.
5. Moghimi SM, Hunter AC, Murray JC. Long-circulating and target-specific nanoparticles: theory to practice. *Pharmacol Rev*. 2001;53(2):283–318.

6. Minko T, Kopeckova P, Pozharov V, Kopecek J. HPMA copolymer bound adriamycin overcomes MDR1 gene encoded resistance in a human ovarian carcinoma cell line. *J Control Release*. 1998;54(2):223–233.

7. Colin de Verdiere A, Dubernet C, Nemati F, Poupon MF, Puisieux F, Couvreur P. Uptake of doxorubicin from loaded nanoparticles in multidrug-resistant leukemic murine cells. *Cancer Chemother Pharmacol*. 1994;33(6):504–508.

8. Weitman SD, Lark RH, Coney LR, et al. Distribution of the folate receptor GP38 in normal and malignant cell lines and tissues. *Cancer Res*. 1992;52(12):3396–3401.

9. Iwasaki Y, Maie H, Akiyoshi K. Cell-specific delivery of polymeric nanoparticles to carbohydrate-tagging cells. *Biomacromolecules*. 2007;8(10):3162–3168.

10. Chen S, Zhang XZ, Cheng SX, Zhuo RX, Gu ZW. Functionalized amphiphilic hyperbranched polymers for targeted drug delivery. *Biomacromolecules*. 2008;9(10):2578–2585.

11. Leamon CP. Folate-targeted drug strategies for the treatment of cancer. *Curr Opin Investig Drugs*. 2008;9(12):1277–1286.

12. Leamon CP, Jackman AL. Exploitation of the folate receptor in the management of cancer and inflammatory disease. *Vitam Horm*. 2008;79:203–233.

13. Low PS, Henne WA, Doorneweerd DD. Discovery and development of folic-acid-based receptor targeting for imaging and therapy of cancer and inflammatory diseases. *Acc Chem Res*. 2008;41(1):120–129.

14. Antony AC. The biological chemistry of folate receptors. *Blood*. 1992;79(11):2807–2820.

15. Lu Y, Low PS. Folate-mediated delivery of macromolecular anticancer therapeutic agents. *Adv Drug Deliv Rev*. 2002;54(5):675–693.

16. Reddy JA, Allagadda VM, Leamon CP. Targeting therapeutic and imaging agents to folate receptor positive tumors. *Curr Pharm Biotechnol*. 2005;6(2):131–150.

17. Saul JM, Annapragada AV, Bellamkonda RV. A dual-ligand approach for enhancing targeting selectivity of therapeutic nanocarriers. *J Control Release*. 2006;114(3):277–287.

18. Sudimack J, Lee RJ. Targeted drug delivery via the folate receptor. *Adv Drug Deliv Rev*. 2000;41(2):147–162.

19. Yao H, Ng SS, Tucker WO, et al. The gene transfection efficiency of a folate-PEI600-cyclodextrin nanopolymer. *Biomaterials*. 2009;30(29):5793–5803.

20. Kim YK, Choi JY, Yoo MK, et al. Receptor-mediated gene delivery by folate-PEG-baculovirus in vitro. *J Biotechnol*. 2007;131(3):353–361.

21. Gabizon A, Horowitz AT, Goren D, et al. Targeting folate receptor with folate linked to extremities of poly(ethylene glycol)-grafted liposomes: in vitro studies. *Bioconjug Chem*. 1999;10(2):289–298.

22. Zhang Y, Li J, Lang M, Tang X, Li L, Shen X. Folate-functionalized nanoparticles for controlled 5-fluorouracil delivery. *J Colloid Interface Sci*. 2011;354(1):202–209.

23. Yanasarn N, Sloat BR, Cui Z. Nanoparticles engineered from lecithin-in-water emulsions as a potential delivery system for docetaxel. *Int J Pharm*. 2009;379(1):174–180.

24. Mosmann T. Rapid colorimetric assay for cellular growth and survival: application to proliferation and cytotoxicity assays. *J Immunol Methods*. 1983;65(1–2):55–63.

25. Danhier F, Lecouturier N, Vroman B, et al. Paclitaxel-loaded PEGylated PLGA-based nanoparticles: in vitro and in vivo evaluation. *J Control Release*. 2009;133(1):11–17.

26. Zhang J, Qian Z, Gu Y. In vivo anti-tumor efficacy of docetaxel-loaded thermally responsive nanohydrogel. *Nanotechnology*. 2009;20(32):325102.

27. Oh KT, Lee ES, Kim D, Bae YH. L-histidine-based pH-sensitive anticancer drug carrier micelle: reconstitution and brief evaluation of its systemic toxicity. *Int J Pharm*. 2008;358(1–2):177–183.

28. Ho JA, Hung CH, Wu LC, Liao MY. Folic acid-anchored PEGgylated phospholipid bioconjugate and its application in a liposomal immuno-diagnostic assay for folic acid. *Anal Chem*. 2009;81(14):5671–5677.

29. Adkins SS, Hobbs HR, Benaissi K, Johnston KP, Poliakoff M, Thomas NR. Stable colloidal dispersions of a lipase-perfluoropolyether complex in liquid and supercritical carbon dioxide. *J Phys Chem B*. 2008;112(15):4760–4769.

30. Hayes ME, Drummond DC, Hong K, Park JW, Marks JD, Kirpotin DB. Assembly of nucleic acid-lipid nanoparticles from aqueous-organic monophases. *Biochim Biophys Acta*. 2006;1758(4):429–442.

31. Ghera BB, Perret F, Chevalier Y, Parrot-Lopez H. Novel nanoparticles made from amphiphilic perfluoroalkyl alpha-cyclodextrin derivatives: preparation, characterization and application to the transport of acyclovir. *Int J Pharm*. 2009;375(1–2):155–162.

32. Sjostrom B, Kronberg B, Carlfors J. A method for the preparation of submicron particles of sparingly water-soluble drugs by precipitation in oil-in-water emulsions. I: influence of emulsification and surfactant concentration. *J Pharm Sci*. 1993;82(6):579–583.

33. Le Garrec D, Gori S, Luo L, et al. Poly(N-vinylpyrrolidone)-block-poly(D,L-lactide) as a new polymeric solubilizer for hydrophobic anticancer drugs: in vitro and in vivo evaluation. *J Control Release*. 2004;99(1):83–101.

34. Shiokawa T, Hattori Y, Kawano K, et al. Effect of polyethylene glycol linker chain length of folate-linked microemulsions loading aclacinomycin A on targeting ability and antitumor effect in vitro and in vivo. *Clin Cancer Res*. 2005;11(5):2018–2025.

35. Yoo HS, Park TG. Folate-receptor-targeted delivery of doxorubicin nano-aggregates stabilized by doxorubicin-PEG-folate conjugate. *J Control Release*. 2004;100(2):247–256.

36. Liu D, Liu F, Liu Z, Wang L, Zhang N. Tumor specific delivery and therapy by double-targeted nanostructured lipid carriers with anti-VEGFR-2 antibody. *Mol Pharm*. 2011;8(6):2291–2301.

37. Zheng D, Li X, Xu H, Lu X, Hu Y, Fan W. Study on docetaxel-loaded nanoparticles with high antitumor efficacy against malignant melanoma. *Acta Biochim Biophys Sin (Shanghai)*. 2009;41(7):578–587.

38. Yang Y, Wang J, Zhang X, Lu W, Zhang Q. A novel mixed micelle gel with thermo-sensitive property for the local delivery of docetaxel. *J Control Release*. 2009;135(2):175–182.

39. Wang X, Yang L, Chen ZG, Shin DM. Application of nanotechnology in cancer therapy and imaging. *CA Cancer J Clin*. 2008;58(2):97–110.

40. Xia W, Low PS. Folate-targeted therapies for cancer. *J Med Chem*. 2010;53(19):6811–6824.

41. Zhao X, Zhao Y, Geng L, et al. Pharmacokinetics and tissue distribution of docetaxel by liquid chromatography-mass spectrometry: evaluation of folate receptor-targeting amphiphilic copolymer modified nanostructured lipid carrier. *J Chromatogr B Analyt Technol Biomed Life Sci*. 2011;879(31):3721–3727.

42. Gref R, Luck M, Quellec P, et al. "Stealth" corona-core nanoparticles surface modified by polyethylene glycol (PEG): influences of the corona (PEG chain length and surface density) and of the core composition on phagocytic uptake and plasma protein adsorption. *Colloids Surf B Biointerfaces*. 2000;18(3–4):301–313.

43. Sinha R, Kim GJ, Nie S, Shin DM. Nanotechnology in cancer therapeutics: bioconjugated nanoparticles for drug delivery. *Mol Cancer Ther*. 2006;5(8):1909–1917.